inorganics

MDPI

Article

Ti-Ce Nanocatalysts for Evaluation in the Photodegradation of Naproxen and Acetaminophen

Adriana Marizcal-Barba [1], Gerardo Vallejo-Espinosa [1], Yéssica V. Contreras-Pacheco [1], Carlos A. Soto-Robles [1], Karina Nava-Andrade [1], María del Camen Leal-Moya [2], Suresh Ghotekar [3], Mamoun Fellah [4], Claudia M. Gomez [5], Osmín Avilés-García [1] and Alejandro Pérez-Larios [1,*]

[1] Nanocatalysis Research Laboratory, Engineering Department, Centro Universitario de los Altos, Universidad de Guadalajara, Tepatitlán de Morelos 47600, Mexico; osmin.aviles@academicos.udg.mx (O.A.-G.)
[2] Department of Centro Universitario de los Altos, University of Guadalajara, Tepatitlán de Morelos 47600, Mexico
[3] Centre for Herbal Pharmacology and Environmental Sustainability, Chettinad Hospital and Research Institute, Chettinad Academy of Research and Education, Kelambakkam 603103, Tamil Nadu, India
[4] Mechanical Engineering Department, Abbes Laghrour-University, Khenchela P.O. Box 1252, 40004, Algeria
[5] Departamento de Química, División de Ciencias Naturales y Exactas, Campus Guanajuato de la Universidad de Guanajuato, Noria Alta s/n, Col. Noria Alta, Guanajuato 36050, Mexico
* Correspondence: alarios@cualtos.udg.mx

Abstract

The pharmaceutical industry is a major source of pollution in wastewater effluents, characterized by chemical residues that are complex and difficult to degrade. Naproxen, a commonly detected drug in sewage effluents, exceeds safe concentrations for aquifers and is highly persistent, posing significant risks to aquatic life and ecosystems. This drug is known to cause long-term side effects in humans, such as gastrointestinal ulcers and nephrosis, associated with frequent and prolonged use. Additionally, the recent pandemic has led to a marked increase in drug consumption over a short period, exacerbating environmental contamination. Titanium dioxide has been extensively used as a photocatalyst in recent decades, proving effective in reducing these emerging pollutants. In this study, TiO_2 doped with cerium was synthesized using the sol–gel method, with cerium concentrations varied at 1, 3, 5, and 10% by weight. The resulting nanocatalysts were characterized through nitrogen physisorption, scanning electron microscopy (SEM), X-ray diffraction (XRD), and UV-Vis diffuse reflectance spectroscopy. Photocatalytic activity was assessed using a UV-Vis spectrophotometer to monitor the degradation of the drugs. XRD analysis confirmed the crystallinity and anatase phase of TiO_2. UV-Vis diffuse reflectance spectra indicated a decrease in bandgap energy of up to 3.00 eV compared to pure TiO_2. The materials demonstrated significant degradation of naproxen (NPX) and acetaminophen (ACTP), both prepared at 30 ppm, over a 6 h reaction period.

Keywords: TiO_2; mixed oxide; photocatalyst; photodegradation

Check for updates

Academic Editor: Antonino Gulino

Received: 20 March 2026
Revised: 20 April 2026
Accepted: 25 April 2026
Published: 1 May 2026

Copyright: © 2026 by the authors. Licensee MDPI, Basel, Switzerland. This article is an open access article distributed under the terms and conditions of the Creative Commons Attribution (CC BY) license.

1. Introduction

The pharmaceutical industry significantly contributes to water pollution, with active pharmaceutical ingredients (APIs) permeating natural water bodies through their production, use, and disposal. This widespread dispersion has classified APIs as emerging pollutants posing global environmental challenges. Research by Beek et al. highlighted the detection of drug residues in 71 countries, identifying a total of 631 drugs and 16 pharmaceutical residues beyond acceptable limits [1,2]. The ecological impact of these residues

includes bacterial resistance to antibiotics and disruption of aquatic life through mechanisms such as fish predation and endocrine disruption, manifesting as feminization of fish populations [3,4].

Naproxen, a widely recognized non-selective nonsteroidal anti-inflammatory drug and a bicyclic propionic acid derivative, exhibits ecosystem toxicity both directly and via its metabolites. Its adverse effects range from bioaccumulation and gastrointestinal issues to renal complications and endocrine disturbances [5]. Similarly, acetaminophen, one of the most commonly used over-the-counter medications, is largely present in wastewater, with human bodies excreting 58–68% of ingested doses [6].

The persistence of pharmaceutical pollutants in aquatic systems has necessitated the development of effective remediation strategies. Traditional methods like adsorption, biological treatments, and membrane-based processes are limited by factors such as sludge production and the need for frequent adsorbent regeneration [7]. Advanced oxidation processes (AOPs), which involve the generation of hydroxyl radicals to break down pollutants into non-harmful substances like water and carbon dioxide, offer a robust alternative. These radicals are produced through various methods, including chemical, electrochemical, and photochemical processes [8].

Photocatalysis, a method leveraging the unique properties of semiconductors like titanium dioxide (TiO_2) and zinc oxide (ZnO), is particularly promising due to its efficiency in generating electron–hole pairs essential for the catalytic breakdown of contaminants. TiO_2 and ZnO are widely recognized semiconductor photocatalysts; however, TiO_2 is preferred due to its superior chemical and photochemical stability under the experimental conditions [9]. TiO_2 exhibits strong resistance to photocorrosion and maintains its structural integrity during prolonged irradiation in aqueous systems [10], whereas ZnO is prone to dissolution and photocorrosion, particularly under acidic or reactive conditions [11]. Although ZnO can exhibit high electron mobility, its practical photocatalytic performance is often limited by its instability in aqueous environments. In contrast, TiO_2, especially in its anatase phase, has been widely reported to exhibit effective charge separation and efficient generation of reactive oxygen species under UV irradiation [12]. Furthermore, TiO_2 is considered the reference photocatalyst, with well-established mechanisms and widely validated modification strategies, which facilitate reproducibility and interpretation of results [13]. It also maintains stable activity over a broad pH range, unlike ZnO, whose performance decreases significantly in acidic environments. Although ZnO may offer advantages such as higher electron mobility or absorption efficiency in specific cases, these are often outweighed by its limited chemical stability [14,15]. Despite the effectiveness of TiO_2 and ZnO, their utility is often hindered by the rapid recombination of these electron–hole pairs. To overcome this limitation, doping TiO_2 with elements such as cerium (Ce) and lanthanum (La) has proven effective. CeO_2, known for its oxygen storage capabilities and redox properties, enhances photocatalytic activity [16].

This study evaluates the efficacy of Ce-TiO_2 nanoparticles in degrading common wastewater contaminants like naproxen (NPX) and acetaminophen (ACTP), focusing on their enhanced photocatalytic properties through the incorporation of cerium.

2. Results and Discussion

2.1. Characterization of Ti-Ce X Photocatalysts

2.1.1. Scanning Electron Microscopy (SEM)

Figure 1 presents the SEM micrographs of the Ti-Ce nanocomposites, where Ti-Ce1, Ti-Ce3, Ti-Ce5, and Ti-Ce10 display semicircular and amorphous morphologies with notable agglomeration. Noteworthy is that agglomeration intensifies with increasing Ce content, suggesting enhanced interaction within the Ti-Ce matrix. This statement is supported by

other research where the presence and increase in metallic species induce morphological changes, including aggregation, particle growth, or the formation of denser structures, which reflect stronger interactions between phases, oxides, or dopants [17,18]. These interactions can be induced by the presence of oxygen vacancies in the matrix, which could enhance the interaction between species [19]. Likewise, the homogeneous incorporation of Ce during the synthesis method can lead to structures with larger aggregates [20].

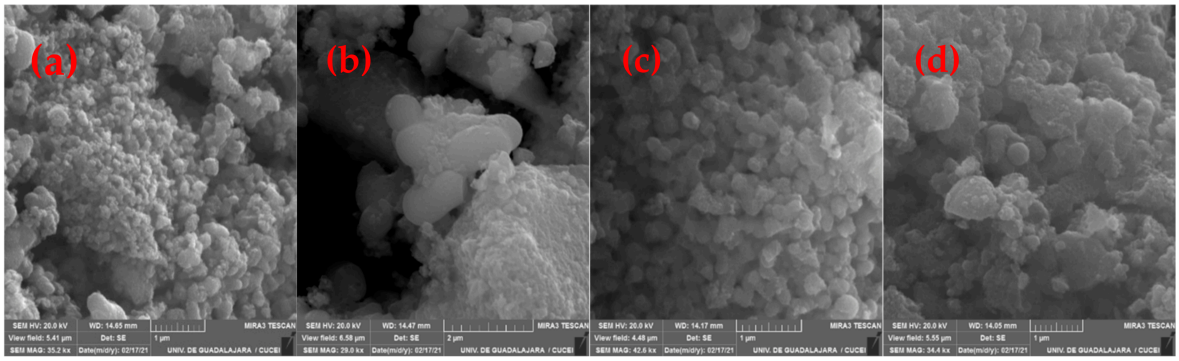


Figure 1. SEM micrographs of the Ti-Ce nanocatalysts, (**a**) Ti-Ce1, (**b**) Ti-Ce3, (**c**) Ti-Ce5 and (**d**) Ti-Ce10.

2.1.2. Nitrogen Physisorption

The nitrogen physisorption analysis illustrated in Figure 2a shows Type IV isotherms with Type H2 hysteresis, indicative of mesoporous materials with quasi-cylindrical pore structures [21,22]. These features suggest variable pore sizes across samples, correlating with the degree of cerium incorporation (Figure 2b) [23,24].

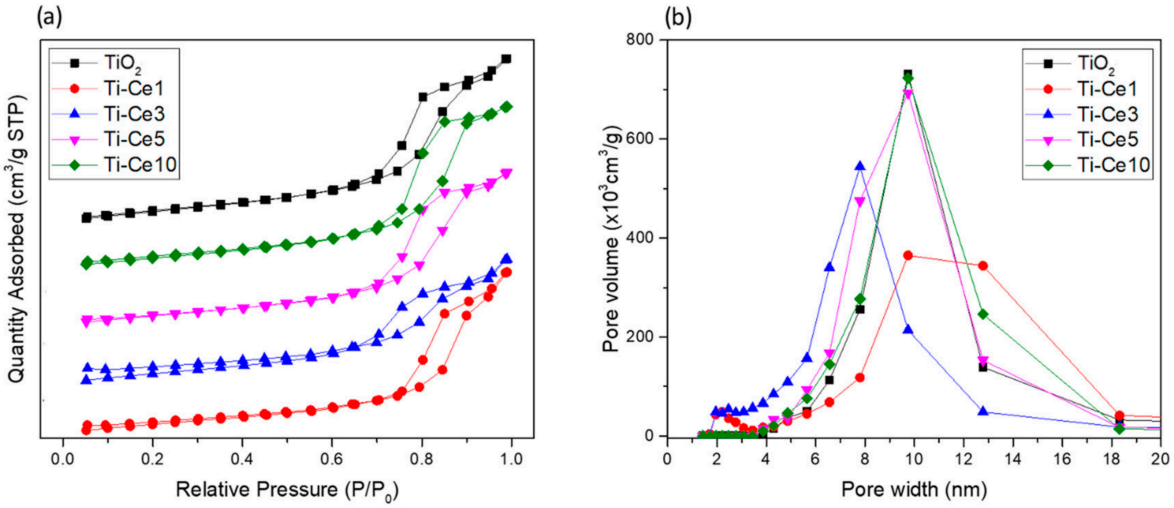


Figure 2. (**a**) Adsorption isotherms and (**b**) pore size distribution of Ti-Ce nanocatalysts.

2.1.3. X-Ray Diffraction (XRD)

XRD analysis confirms only the presence of the TiO_2 anatase phase with a tetragonal structure, evident from diffraction peaks at 2θ values corresponding to various crystal planes, as outlined in JCPDS No. 00-001-0562. As can be seen in Figure 3, no additional peaks attributed to cerium oxides were observed. This may be because the cerium species were well distributed within the crystalline structure of TiO_2 [25]. Even with high Ce concentrations (up to 10 wt.%), no significant peak shifts were observed, indicating that Ce cations could integrate into the TiO_2 matrix without altering its crystallographic structure significantly [26]. The intensity of the diffraction peak (101) decreases with increasing

cerium content (Figure 3b), which is related to the fact that these metallic species could inhibit crystal growth (see Table 1) [27].

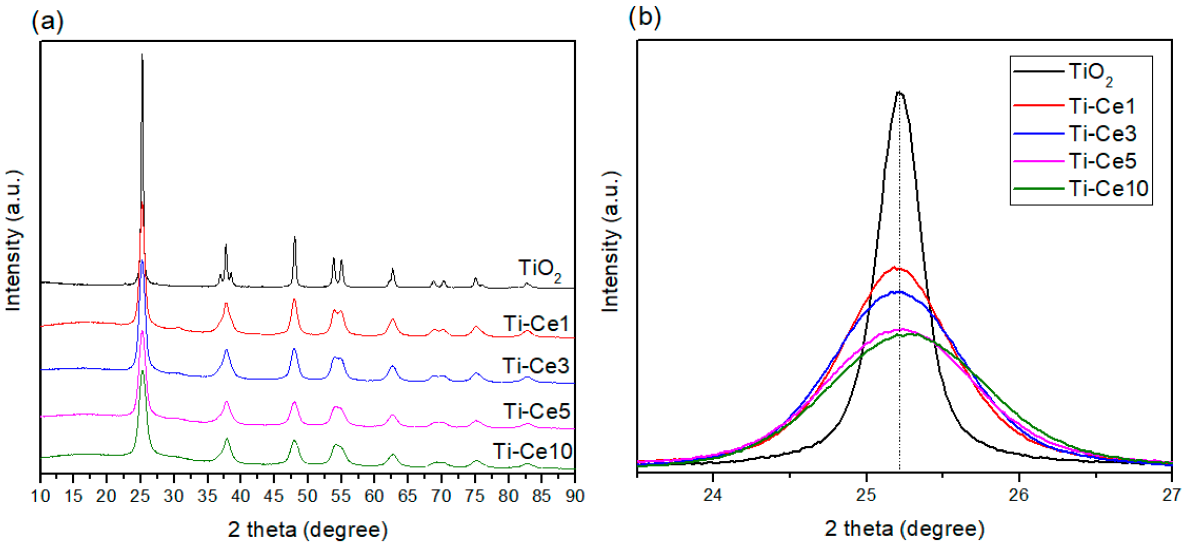


Figure 3. (**a**) X-ray diffractograms and (**b**) diffraction profiles on (1 0 1) plane of Ti-Ce catalysts.

Table 1. Bandgap energy (Eg), crystallite size, d-spacing values and textural properties of Ti-Ce samples.

Samples	BET (m^2/g)	Pore Diameter (nm)	Cell Parameter, a (Å)	Average Size Particle (nm)	E_g (eV)
Ti-Ce1	89.1	15.96	3.527	15 ± 2	3.28
Ti-Ce3	77.8	12.73	3.528	12 ± 1	3.16
Ti-Ce5	111.6	12.59	3.523	15 ± 3	3.03
Ti-Ce10	115.7	12.73	3.520	16 ± 2	3.00
TiO_2	64.0	6.5	3.530	32 ± 6	3.24

2.1.4. UV–Visible Spectroscopy

Figure 4 depicts the UV-Vis absorption spectra and band gap energies, where a shift towards the red region (from 3.00 to 3.24 eV) is observed for the Ti-Ce nanocatalysts compared to pure TiO_2 [28]. This shift suggests a modification in the bandgap due to Ce doping, affecting the electronic properties of TiO_2 [29,30].

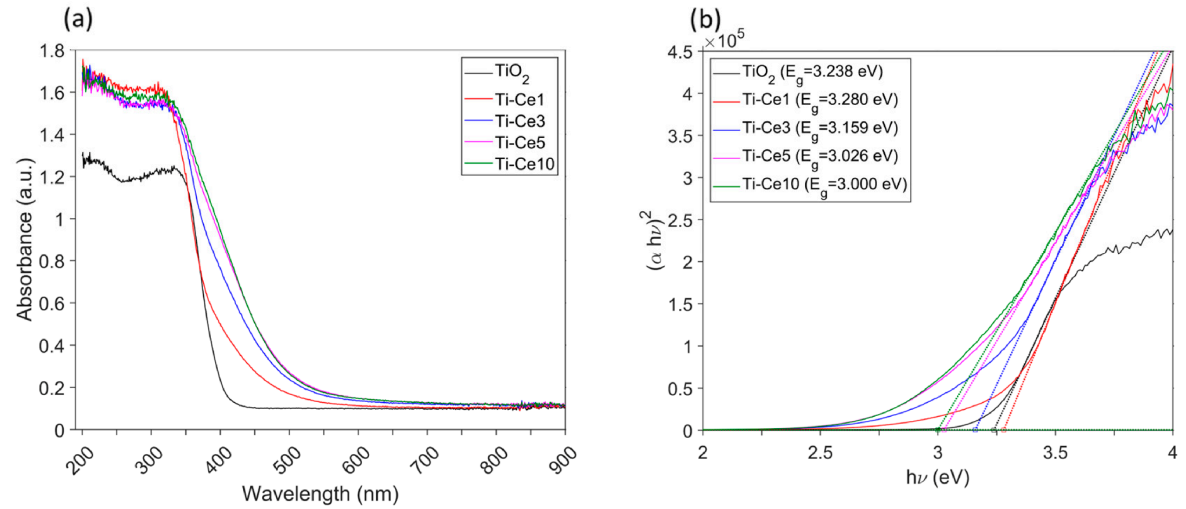


Figure 4. (**a**) Absorption spectra and (**b**) band gap energies (Tauc plots) of Ti-Ce nanocatalysts.

2.1.5. Transmission Electron Microscopy (TEM)

TEM analyzes (Figure 5) reveal nanoglobular and other nanostructures within the nanocatalysts, confirming the homogeneous distribution of Ce within the titania matrix, which is critical for effective photocatalytic activity [31]. It can be observed that the presence of cerium metallic species in TiO_2 decreases the crystalline particle size, which is in agreement with the XRD results. Table 2 shows the percentage by weight content of the species present in all synthesized materials, and these values are very close to the theoretical ones.

Table 2. Percentage by weight of nanocatalysts.

Nanocatalyst	Content %		
	Ti	O	Ce
TiO_2	60	40	-
Ti-Ce1	59	36	2
Ti-Ce3	63	29	4
Ti-Ce5	52	39	6
Ti-Ce10	51	39	10

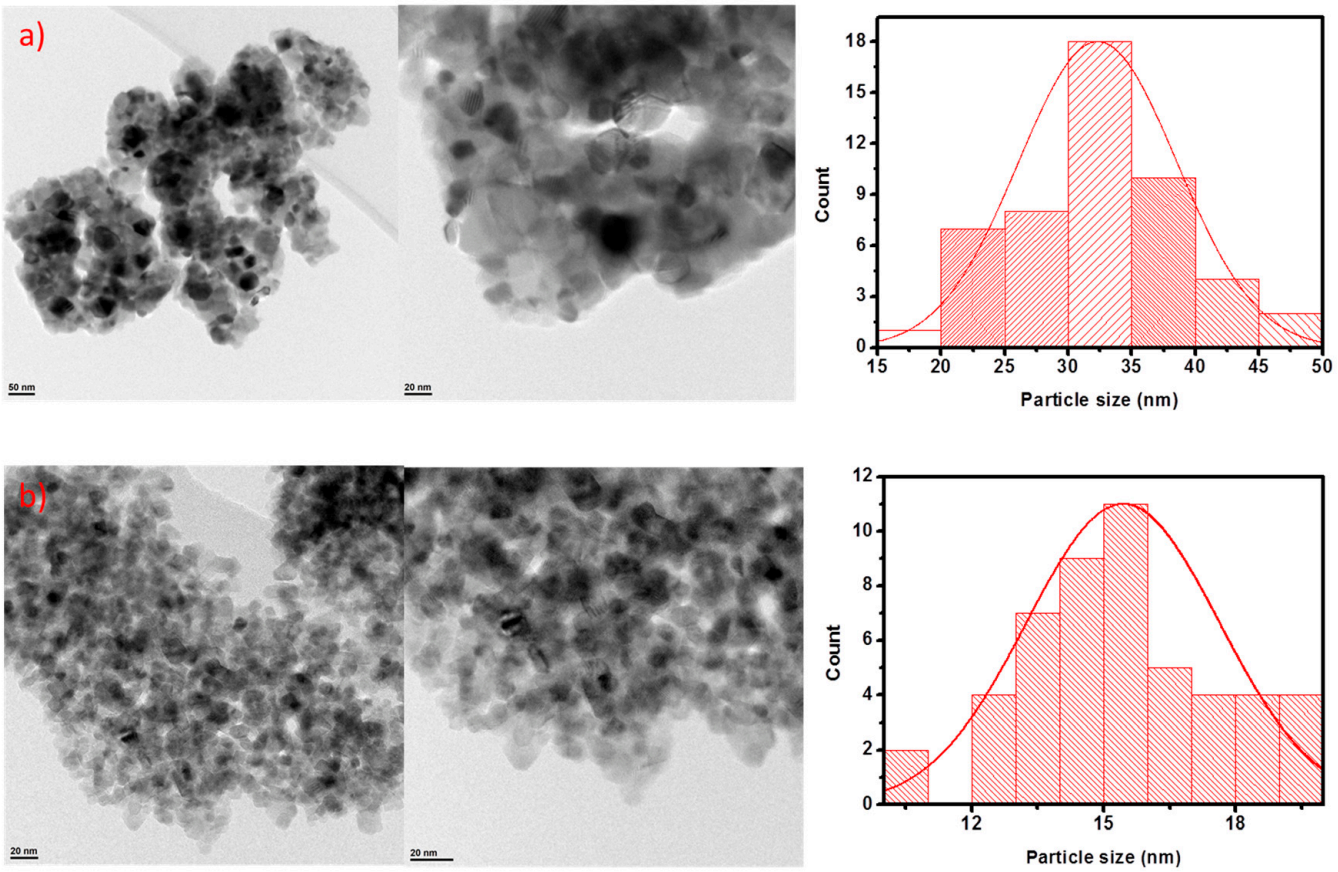


Figure 5. *Cont.*

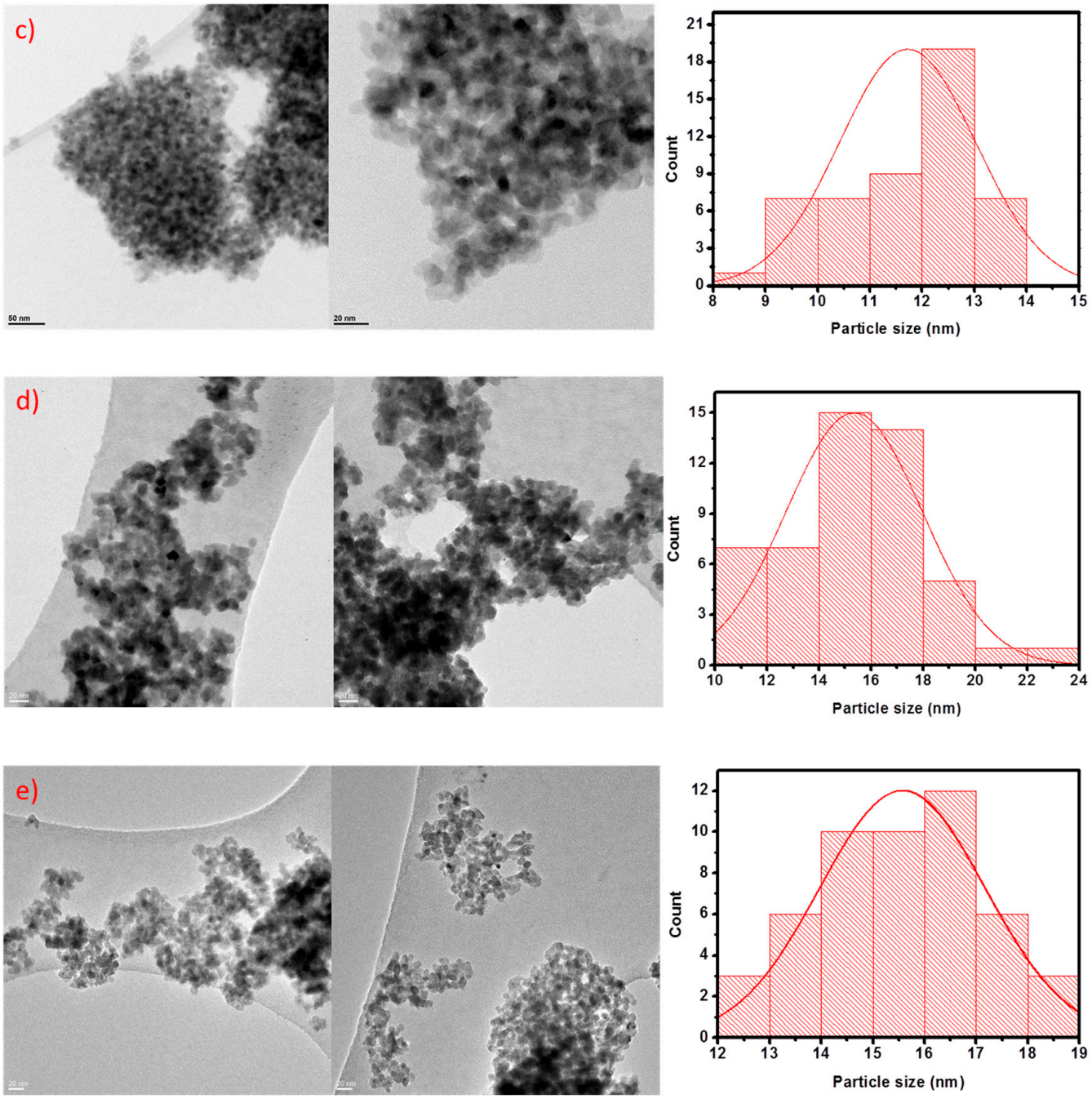


Figure 5. TEM images and particle size distribution of photocatalysts. (**a**) TiO_2, (**b**) Ti-Ce1, (**c**) Ti-Ce3, (**d**) Ti-Ce5 and (**e**) Ti-Ce10.

2.2. Photocatalytic Activity

The photocatalytic efficiency was quantified by monitoring the degradation of acetaminophen (ACTP) and naproxen (NPX) (Figure 6) [31]. The results show that Ti-Ce1 exhibits the highest degradation efficiency, potentially due to optimal Ce doping enhancing hydroxyl radical production, which is crucial for effective pharmaceutical degradation in wastewater treatments [32,33].

As can be seen in Figure 6, the degradation efficiency is observed under photocatalytic conditions using Ti-Ce 1% nanocatalyst, emphasizing their superior performance compared to photolysis under non-catalytic conditions. A notable reduction in degradation is seen, reinforcing the importance of catalyst and reaction conditions in achieving optimal performance, which highlights the critical role of Ti-Ce in accelerating the degradation

process. This comparative analysis underscores the efficiency of the Ti-Ce nanocatalysts in environmental remediation, with ACTP and NPX exhibiting similar trends, though ACTP generally shows slightly higher degradation efficiencies.

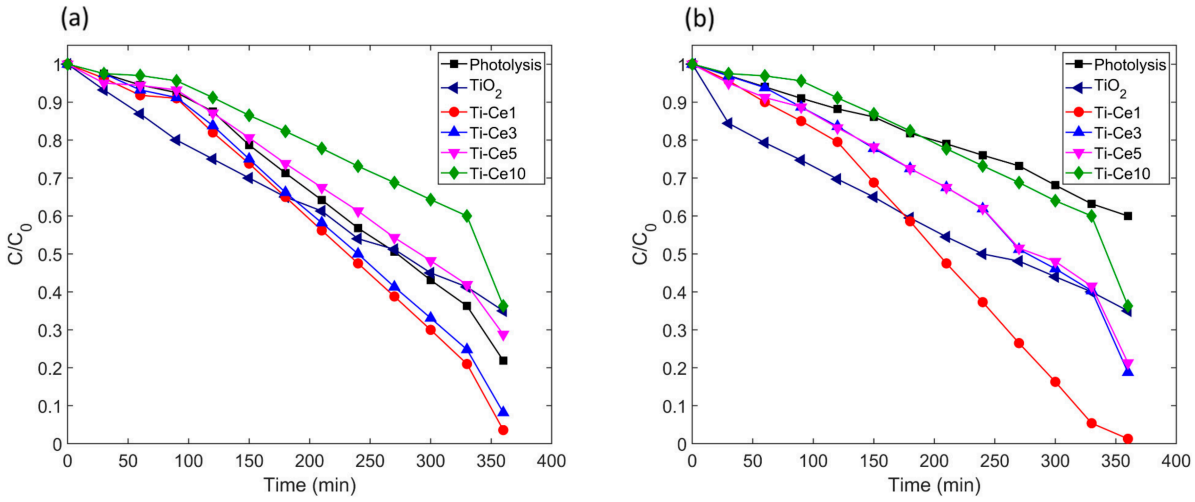


Figure 6. Degradation of Ti-Ce nanocatalysts, (**a**) ACTP and (**b**) NPX.

The photocatalytic degradation mechanism of naproxen and acetaminophen using Ce-doped TiO_2 can be described based on the generation and participation of reactive oxygen species under irradiation. The excitation of the semiconductor produces electron–hole pairs (e^-/h^+) (Equation (1)), where the incorporation of Ce introduces intermediate energy states associated with the Ce^{4+}/Ce^{3+} redox couple, which act as electron trapping centers, promoting charge separation and reducing recombination [34]. The photogenerated electrons react with dissolved oxygen to form superoxide radicals ($O_2^{\cdot -}$) (Equation (2)), while the holes oxidize water or surface hydroxyl groups to generate hydroxyl radicals (·OH) (Equation (3)). These highly oxidative species are responsible for the degradation of pharmaceutical compounds through hydroxylation, aromatic ring cleavage, and progressive oxidation leading to partial or complete mineralization (Equation (4)), in agreement with mechanisms reported for doped TiO_2 photocatalytic systems [35–37]. This description represents the excitation of the semiconductor, the role of Ce as an electron trap, and the formation of reactive species responsible for contaminant degradation. When the dopant content is high, the cerium metal species become recombination sites for photogenerated positive holes, as they are negatively charged by acting as a trap for photogenerated electrons, thus decreasing photocatalytic activity.

$$TiO_2/Ce + h\nu \rightarrow e^- + h^+ \quad (1)$$

$$e^- + O_2 \rightarrow O_2^{\cdot -} \quad (2)$$

$$h^+ + H_2O \rightarrow \cdot OH + H^+ \quad (3)$$

$$\cdot OH/O_2^{\cdot -} + \text{Drug} \rightarrow CO_2 + H_2O + \text{Intermediate products} \quad (4)$$

Furthermore, it can be observed that despite the presence of cerium doping species and the band-gap reduction, the catalytic photodegradation of both drugs is favored under UV irradiation at 254 nm. This is related, firstly, to the appropriate concentration of dopant that prevents the recombination of the photogenerated charges and, secondly, to the generation

of hydroxyl radicals from the hydrogen peroxide formed during the photocatalytic process due to the interaction with a sufficiently energetic radiation source [38].

Figure 7 shows the kinetics of Ti-Ce nanocatalysts for the degradation of ACTP (a) and NPX (b), showing the effect of different nanocomposite concentrations (1%, 3%, 5%, and 10%) compared to photolysis as a control. In both cases, photolysis exhibits the lowest degradation rates, highlighting the limited impact of direct photodegradation without the catalyst. The degradation rates increase significantly with lower nanocatalyst concentrations, showing markedly improved performance due to the greater availability of active catalytic sites [39]. ACTP shows faster degradation kinetics across all concentrations compared to NPX, suggesting differences in the susceptibility of the compounds to photocatalytic breakdown, likely influenced by molecular structure or interaction with the catalyst. Ti-Ce nanocatalysts enhance the degradation process by generating reactive oxygen species under irradiation, with the results emphasizing their potential as efficient photocatalysts for environmental remediation. The data also suggest that doping concentration may provide optimal performance, balancing efficiency and material used [40,41].

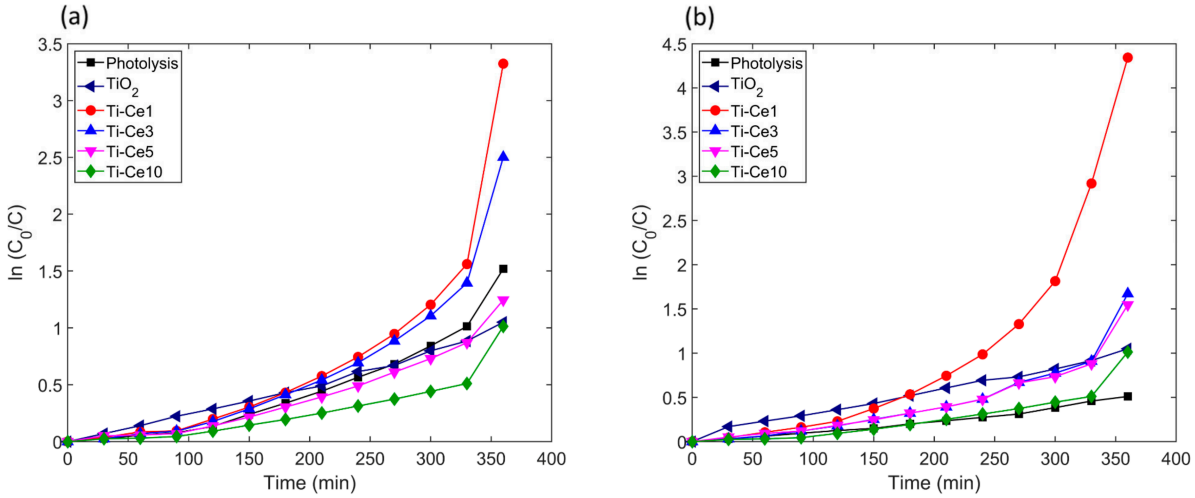


Figure 7. Kinetics of Ti-Ce nanocatalysts, (**a**) ACTP and (**b**) NPX.

3. Materials and Methods

3.1. Synthesis

The Ce-TiO_2 nanocatalysts were synthesized via the sol–gel method. In a three-neck flask, a mixture of ethyl alcohol and water at an 8:1 ratio was prepared, dissolving cerium nitrate to achieve cerium concentrations of 1%, 3%, 5%, and 10%. Solvent composition and the water-to-alkoxide molar ratio (R = [H_2O]/[alkoxide]) controlled the hydrolysis and condensation kinetics in TiO_2 sol–gel systems. Increasing R accelerates hydrolysis and affects nucleation and particle size, while moderate values (R ≈ 4–16) favor stable and homogeneous sols [42–44]. In this work, an ethanol/water mixture (8:1, v/v) was used to control the reaction. The use of an alcohol/water mixture moderated the hydrolysis rate of titanium alkoxides by reducing the effective water activity and improving phase compatibility, preventing uncontrolled precipitation and enabling a more uniform sol–gel process. This allowed a more controlled system and reproducible TiO_2 properties.

Subsequently, the mixture was heated to 70 °C, and titanium butoxide was added dropwise. The reaction was maintained under constant stirring and temperature for 24 h. Post-reaction, the material was dried at 100 °C, ground in an agate mortar, and finally calcined at 500 °C for 5 h with a heating ramp of 2 °C/min.

3.2. Characterization Techniques

3.2.1. Scanning Electron Microscopy (SEM)

A TESCAN MIRA3 microscope (Brno, Czech Republic) was utilized at 20.0 KV to achieve 30 to 60 kx magnification.

3.2.2. Nitrogen Physisorption

Conducted using a Micromeritics TriStar II Plus (Norcross, GA, USA) to assess adsorption isotherms and specific surface area via the BET method, and pore size distribution via the BJH method.

3.2.3. X-Ray Diffraction (XRD)

X-ray diffraction studies were carried out in Panalytical equipment, empyrean model (Malvern, UK) with Cu Kα radiation (λ = 0.154 nm), with a diffraction angle (2θ) from 10 to 90°, using a step of 0.03° and a time 3 s per step.

3.2.4. UV–Visible Spectroscopy

Diffuse reflectance spectra were obtained with a Shimadzu UV-2600 spectrophotometer (Kyoto, Japan), integrated with an integrating sphere. The spectra were analyzed using the Kubelka–Munk function to calculate the extinction coefficient (α), across wavelengths from 900 to 190 nm.

3.2.5. Transmission Electron Microscopy (TEM)

High-resolution imaging was done using a TITAN Cube 60-300 (FEI Company, Zaragoza, Spain) with a spherical aberration corrector at 80 kV.

3.2.6. Photocatalytic Activity Assessment

The photocatalytic degradation of acetaminophen and naproxen was tested in a 400 mL reactor containing 350 mL of the solution, with consistent agitation and air injection at 1 mg/min. The solution's exposure to UV light varied by wavelength (254 nm, 356 nm, and solar irradiation > 400 nm) according to the Ce-TiO_2 composition (1, 3, 5, and 10 wt.%). Degradation kinetics were monitored by measuring the drug concentration at specific wavelengths (243 nm for acetaminophen and 271 nm for naproxen) using a Shimadzu UV-2600 spectrophotometer.

4. Conclusions

The TiO_2 and Ce-TiO_2 photocatalysts were successfully synthesized by the sol–gel method. Nanocatalysts show photodegradation activity because the Ce distribution on the TiO_2 surface and some $Ce^{4+/3+}$ cations in the TiO_2 matrix can improve the material's surface redox properties, which facilitates the mobility of the photogenerated charges during photocatalytic activity. The effect of Ce dose on nanocatalysts could be related to the higher adsorption, and the 4f electron transition of $Ce^{4+/3+}$ ions.

Characterization of the material was successfully achieved. All these results confirmed the presence of the more active anatase crystalline phase of TiO_2. There was also evidence of the expected weight percentage values of each species present in the catalysts, calculated during the synthesis of the materials. The effect of the Ce was observed in the TEM images, in the modification of the particle size, which can be attributed to the presence of Ce-O-Ti bonds that inhibit the growth of crystals.

The best degradation efficiency was achieved with a low amount of cerium by reducing the recombination rate under UV radiation.

Author Contributions: Conceptualization, S.G., M.F. and A.P.-L.; methodology, G.V.-E., M.d.C.L.-M. and Y.V.C.-P.; validation, S.G., M.F. and M.d.C.L.-M.; formal analysis, K.N.-A., C.A.S.-R. and O.A.-G.; investigation, A.M.-B., M.d.C.L.-M. and C.M.G.; data curation, A.M.-B., G.V.-E. and C.M.G.; writing—original draft preparation, C.A.S.-R., K.N.-A. and O.A.-G.; writing—review and editing, S.G., M.F., Y.V.C.-P. and A.P.-L.; supervision, G.V.-E.; project administration, A.P.-L. All authors have read and agreed to the published version of the manuscript.

Funding: This research received no external funding.

Institutional Review Board Statement: Not applicable.

Informed Consent Statement: Not applicable.

Data Availability Statement: The original contributions presented in this study are included in the article. Further inquiries can be directed to the corresponding author.

Acknowledgments: Adriana Marizcal-Barba and Gerardo Vallejo-Espinosa thank CONAHCYT for the scholarship received.

Conflicts of Interest: The authors declare no conflicts of interest.

References

1. Wilkinson, J.L.; Boxall, A.B.A.; Kolpin, D.W.; Leung, K.M.Y.; Lai, R.W.S.; Galbán-Malagón, C.; Adell, A.D.; Mondon, J.; Metian, M.; Marchant, R.A.; et al. Pharmaceutical pollution of the world's rivers. *Proc. Natl. Acad. Sci. USA* **2022**, *119*, e2113947119. [CrossRef]
2. Aus Der Beek, T.; Weber, F.-A.; Bergmann, A.; Hickmann, S.; Ebert, I.; Hein, A.; Küster, A. Pharmaceuticals in the environment—Global occurrences and perspectives. *Environ. Toxicol. Chem.* **2016**, *35*, 823–835. [CrossRef] [PubMed]
3. Canan-Rochenbach, G.; Barreiros, M.A.; Lima, A.O.; Bauda, P.; Sanches-Simões, E.; Pimentel-Almeida, W.; Ariente-Neto, R.; Somensi, C.A.; Almeida, T.C.; Corrêa, R.; et al. Characterization of bacterial resistance in treated hospital wastewater. *Environ. Technol.* **2024**, *45*, 120–128. [CrossRef]
4. Azizi-Lalabadi, M.; Pirsaheb, M. Investigation of steroid hormone residues in fish: A systematic review. *Process Saf. Environ. Prot.* **2021**, *152*, 14–24. [CrossRef]
5. Wojcieszyńska, D.; Guzik, U. Naproxen in the environment: Its occurrence, toxicity to nontarget organisms and biodegradation. *Appl. Microbiol. Biotechnol.* **2020**, *104*, 1849–1857. [CrossRef]
6. Ahmadzadeh, S.; Dolatabadi, M. Removal of acetaminophen from hospital wastewater using electro-Fenton process. *Environ. Earth Sci.* **2018**, *77*, 53. [CrossRef]
7. Eniola, J.O.; Kumar, R.; Barakat, M.A.; Rashid, J. A review on conventional and advanced hybrid technologies for pharmaceutical wastewater treatment. *J. Clean. Prod.* **2022**, *356*, 131826. [CrossRef]
8. Mashuri, S.I.S.; Ibrahim, M.L.; Kasim, M.F.; Mastuli, M.S.; Rashid, U.; Abdullah, A.H.; Islam, A.; Mijan, N.A.; Tan, Y.H.; Mansir, N.; et al. Photocatalysis for organic wastewater treatment: From the basis to current challenges for society. *Catalysts* **2020**, *10*, 1260. [CrossRef]
9. Souza, R.P.; Freitas, T.K.; Domingues, F.S.; Pezoti, O.; Ambrosio, E.; Ferrari-Lima, A.M.; Garcia, J.C. Photocatalytic activity of TiO_2, ZnO and Nb_2O_5 applied to degradation of textile wastewater. *J. Photochem. Photobiol. A Chem.* **2016**, *329*, 9–17. [CrossRef]
10. Coronado, J.M.; Hernández-Alonso, M.D. The Keys of Success: TiO_2 as a Benchmark Photocatalyst. In *Design of Advanced Photocatalytic Materials for Energy and Environmental Applications*; Coronado, J.M., Fresno, F., Hernández-Alonso, M.D., Portela, R., Eds.; Springer: London, UK, 2013; pp. 85–101. [CrossRef]
11. Elumalai, N.; Prabhu, S.; Selvaraj, M.; Silambarasan, A.; Navaneethan, M.; Harish, S.; Ramu, P.; Ramesh, R. Enhanced photocatalytic activity of ZnO hexagonal tube/r-GO composite on degradation of organic aqueous pollutant and study of charge transport properties. *Chemosphere* **2022**, *291*, 132782. [CrossRef]
12. Kamel, A.H.; Abd-Rabboh, H.S.M.; El-Fattah, A.A.; Stambouli, G.B.; Adeida, L. Metal oxides and their composites for the remediation of organic pesticides: Advanced photocatalytic and adsorptive solutions. *RSC Adv.* **2025**, *15*, 6875–6901. [CrossRef]
13. Chen, X.; Mao, S.S. Titanium Dioxide Nanomaterials: Synthesis, Properties, Modifications, and Applications. *Chem. Rev.* **2007**, *107*, 2891–2959. [CrossRef] [PubMed]
14. Lam, S.M.; Sin, J.C.; Abdullah, A.Z.; Mohamed, A.R. Transition metal oxide loaded ZnO nanorods: Preparation, characterization and their UV–vis photocatalytic activities. *Sep. Purif. Technol.* **2014**, *132*, 378–387. [CrossRef]
15. Jaramillo-Páez, C.; Sánchez-Cid, P.; Navío, J.A.; Hidalgo, M.C. A comparative assessment of the UV-photocatalytic activities of ZnO synthesized by different routes. *J. Environ. Chem. Eng.* **2018**, *6*, 7161–7171. [CrossRef]
16. Martos, M.; Julián-López, B.; Folgado, J.V.; Cordoncillo, E.; Escribano, P. Sol–Gel Synthesis of Tunable Cerium Titanate Materials. *Eur. J. Inorg. Chem.* **2008**, *2008*, 3163–3171. [CrossRef]

17. Islam, N.; Fayaz, A.; Hossain, M.I.; Hossain, M.; Hosen, N.; Singha, N.R.; Maktedar, S.S.; Akermi, M.; Hassani, R.; Hasnat, M.A. Imidazole-assisted water splitting: A novel approach to hydrogen evolution reaction over cerium doped titanium oxide composite. *Int. J. Hydrogen Energy* **2026**, *227*, 154519. [CrossRef]
18. Xu, X.; Huang, Q.; Wu, Y.; Zeng, Y.; Zhang, F.; Zhong, Z.; Xing, W. Surface design of V_2O_5–CeO_2–TiO_2/SiC catalytic membrane for high-efficiency synergistic removal of NO and dust. *J. Membr. Sci.* **2026**, *751*, 125532. [CrossRef]
19. Zhang, X.; Wang, Y.; Liao, J.; Wang, J.; Chang, L.; Bao, W. Oxygen vacancy regulation on Cu-Zn oxides with Ce doping for enhancing ultra-deep removing of thiophene. *Fuel* **2024**, *375*, 132607. [CrossRef]
20. Jiang, Y.; Zheng, Y.; Shan, C.; Hou, N.; Wang, H.; Jia, Q.; Han, R.; Liu, Q.; Wang, W. Engineering poisoning-resistant $Ce_{0.8}La_{0.2}Ox$ catalysts via TiO_2 modification for enhanced CS_2 hydrolysis. *Appl. Catal. B Environ. Energy* **2026**, *383*, 126056. [CrossRef]
21. Pérez-Larios, A.; Torres-Ramos, I.; Zanella, R.; Rico, J.L. Ti-Co mixed oxide as photocatalysts in the generation of hydrogen from water. *Int. J. Chem. React. Eng.* **2022**, *20*, 129–140. [CrossRef]
22. Farcy, A.; Mathy, M.; Lejeune, L.; Eloy, P.; Hermans, S.; Drogui, P.; Mahy, J.G. Ce_2O_3 and TiO_2 p-n heterojunction for enhanced degradation of p-nitrophenol under visible light. *J. Photochem. Photobiol. A Chem.* **2025**, *463*, 116284. [CrossRef]
23. Limón-Rocha, I.; Guzmán-González, C.A.; Anaya-Esparza, L.M.; Romero-Toledo, R.; Rico, J.L.; González-Vargas, O.A.; Pérez-Larios, A. Effect of the Precursor on the Synthesis of ZnO and Its Photocatalytic Activity. *Inorganics* **2022**, *10*, 16. [CrossRef]
24. Ruíz-Santoyo, V.; Marañon-Ruiz, V.F.; Romero-Toledo, R.; Vargas, O.A.G.; Pérez-Larios, A. Photocatalytic degradation of rhodamine b and methylene orange using TiO_2-ZrO_2 as nanocomposite. *Catalysts* **2021**, *11*, 1035. [CrossRef]
25. de la Garza, A.R.; Zeghioud, H.; Benítez-Rico, A.; Romero-Nuñez, A.; Djelal, H.; Chávez-Miyauchi, T.E.; Guillén-Cervantes, J.Á. Visible LED active photocatalyst based on cerium doped titania for Rhodamine B degradation: Radical's contribution, stability and response surface methodology optimization. *Mater. Sci. Semicond. Process.* **2024**, *176*, 108349. [CrossRef]
26. Kang, H.; Yuan, H.; Zhang, H.; Kong, X.; Wang, Y.; Zhang, S.; Liu, J. Enhanced charge separation in Ce-doped TiO_2 heterophase junctions: Mechanistic insights from in-situ XPS and ATR-FTIR studies. *J. Solid State Chem.* **2026**, *355*, 125790. [CrossRef]
27. Avilés-García, O.; Espino-Valencia, J.; Romero, R.; Rico-Cerda, J.L.; Arroyo-Albiter, M.; Natividad, R. W and Mo doped TiO_2: Synthesis, characterization and photocatalytic activity. *Fuel* **2017**, *198*, 31–41. [CrossRef]
28. Khan, H.; Alalm, M.G.; Lalonde-Lavoie, M.; Ordonez, M.F.; Sartirana, M.; Giordana, A.; Cerrato, G.; Bianchi, C.L.; Boffito, D.C. Photocatalytic degradation of NOx and ethanol in the gas phase by spray dried Ce-TiO_2. *J. Environ. Chem. Eng.* **2021**, *9*, 106813. [CrossRef]
29. Keerthana, S.P.; Yuvakkumar, R.; Ravi, G.; Hong, S.I.; Al-Sehemi, A.G.; Velauthapillai, D. Fabrication of Ce doped TiO_2 for efficient organic pollutants removal from wastewater. *Chemosphere* **2022**, *293*, 133540. [CrossRef]
30. Jamil, A.; Sawaira, T.; Ali, A.; Awais, M.; Habib, A.; Hussain, T.; Sharif, A.; Iqbal, N.; Afzal, A. Ce-TiO_2 nanoparticles with surface-confined Ce^{3+}/Ce^{4+} redox pairs for rapid sunlight-driven elimination of organic contaminants from water. *Environ. Nanotechnol. Monit. Manag.* **2024**, *21*, 100946. [CrossRef]
31. Marizcal-Barba, A.; Sanchez-Burgos, J.A.; Zamora-Gasga, V.; Larios, A.P. Study of the Response Surface in the Photocatalytic Degradation of Acetaminophen Using TiO_2. *Photochem* **2022**, *2*, 225–236. [CrossRef]
32. Hao, X.; Tian, J.; Zhao, Y.; Jing, T.; Zheng, Y.; Lu, Z. Photocatalytic degradation of tetracycline over Ce-doped TiO_2@SiO_2@Fe_3O_4 magnetic material. *New J. Chem.* **2023**, *47*, 5939–5945. [CrossRef]
33. Tiwari, S.; Bhatt, J.P.; Ameta, S.C. Photocatalytic Degradation of Carbofuran with Cerium Doped TiO_2 under UV-Irradiation. *Res. J. Chem. Environ.* **2025**, *2*, 114. [CrossRef]
34. Gadge, A.S.; Janbandhu, S.Y.; Gedam, R.S. Exploring the photocatalytic and antibacterial activity of Ce-doped TiO_2 nanoparticles with remarkable self-cleaning superhydrophilic surface for outdoor application. *Ceram. Int.* **2025**, *51*, 602–611. [CrossRef]
35. Ahmadpour, N.; Nowrouzi, M.; Avargani, V.M.; Sayadi, M.H.; Zendehboudi, S. Design and optimization of TiO_2-based photocatalysts for efficient removal of pharmaceutical pollutants in water: Recent developments and challenges. *J. Water Process Eng.* **2024**, *57*, 104597. [CrossRef]
36. Velempini, T.; Prabakaran, E.; Pillay, K. Recent developments in the use of metal oxides for photocatalytic degradation of pharmaceutical pollutants in water—A review. *Mater. Today Chem.* **2021**, *19*, 100380. [CrossRef]
37. Ruziwa, D.T.; Oluwalana, A.E.; Mupa, M.; Meili, L.; Selvasembian, R.; Nindi, M.M.; Sillanpaa, M.; Gwenzi, W.; Chaukura, N. Pharmaceuticals in wastewater and their photocatalytic degradation using nano-enabled photocatalysts. *J. Water Process Eng.* **2023**, *54*, 103880. [CrossRef]
38. Avilés-García, O.; Mendoza-Zepeda, A.; Regalado-Méndez, A.; Espino-Valencia, J.; Martínez-Vargas, S.L.; Romero, R.; Natividad, R. Photo-Oxidation of Glycerol Catalyzed by Cu/TiO_2. *Catalysts* **2022**, *12*, 835. [CrossRef]
39. Bhosale, M.G.; Sutar, R.S.; Londhe, S.S.; Patil, M.K. Sol–gel method synthesized Ce-doped TiO_2 visible light photocatalyst for degradation of organic pollutants. *Appl. Organomet. Chem.* **2022**, *36*, e6586. [CrossRef]
40. Hu, Y.; Yang, T.; Zhou, W.; Huang, Z.; Duan, X.; Yu, M.; Zhou, W.; Lin, F.; Li, D.; Xu, J. Abundant oxygen vacancies Ce-doped TiO_2 supported Pt nanoparticles for high-efficiency photoelectrocatalytic methanol oxidation. *J. Alloys Compd.* **2025**, *1022*, 179975. [CrossRef]

41. Singh, D.; Khan, F.; Jain, V.K.; Bhattacharya, S. Efficient photodegradation of methylene blue dye using cerium-doped titanium dioxide (Ce@TiO_2) photocatalyst under visible light irradiation. *J. Indian Chem. Soc.* **2024**, *101*, 101356. [CrossRef]
42. Amiri, A. Solid-phase microextraction-based sol–gel technique. *TrAC Trends Anal. Chem.* **2016**, *75*, 57–74. [CrossRef]
43. Kojima, T.; Sugimoto, T. Formation Mechanism of Amorphous TiO_2 Spheres in Organic Solvents 3. Effects of Water, Temperature, and Solvent Composition. *J. Phys. Chem. C* **2008**, *112*, 18445–18454. [CrossRef]
44. Yang, J.; Tian, L.; Li, B.; Guo, Y.; Zhang, Y. Effect of water content on the performance and structure of nanosized TiO_2 sol. *Ferroelectrics* **2019**, *547*, 1–9. [CrossRef]

Disclaimer/Publisher's Note: The statements, opinions and data contained in all publications are solely those of the individual author(s) and contributor(s) and not of MDPI and/or the editor(s). MDPI and/or the editor(s) disclaim responsibility for any injury to people or property resulting from any ideas, methods, instructions or products referred to in the content.